

# Nonlinear thermotics: nonlinearity enhancement and harmonic generation in thermal metasurfaces

Gaole Dai<sup>1</sup>, Jin Shang<sup>1</sup>, Ruizhe Wang<sup>1</sup>, and Jiping Huang<sup>1,2,a</sup>

<sup>1</sup> Department of Physics, State Key Laboratory of Surface Physics, and Key Laboratory of Micro and Nano Photonic Structures (MOE), Fudan University, Shanghai 200433, P.R. China

<sup>2</sup> Collaborative Innovation Center of Advanced Microstructures, Nanjing 210093, P.R. China

Received 20 October 2017 / Received in final form 5 December 2017

Published online 29 March 2018 – © EDP Sciences, Società Italiana di Fisica, Springer-Verlag 2018

**Abstract.** We propose and investigate a class of structural surfaces (metasurfaces). We develop the perturbation theory and the effective medium theory to study the thermal properties of the metasurface. We report that the coefficient of temperature-dependent (nonlinear) item in thermal conductivity can be enhanced under certain conditions. Furthermore, the existence of nonlinear item helps to generate high-order harmonic frequencies of heat flux in the presence of a heat source with periodic temperature. This work paves a different way to control and manipulate the transfer of heat, and it also makes it possible to develop nonlinear thermotics in the light of nonlinear optics.

## 1 Introduction

How to control the behavior of heat transfer is a crucial issue as people are faced with serious energy shortage. The theoretical and experimental designs of thermal metamaterial have been quickly developing these years to manipulate heat flow according to human wills. As a result, thermal metamaterials or meta-devices [7,8,9,10,11,12,13,14,15,16,17,1,2,3,4,5,6], such as thermal diodes [16,1], thermal transistors [2,5], thermal logic gates [3], thermal memory [6], thermal cloaks [7,8,9,10,11,12,13,14,16], and thermal sensors [15], have come to appear and played an important role in satisfying this demand. Actually, quite a lot of thermal metamaterials are designed based on the nonlinearity of heat conduction [16,17,1,2,3], meaning that the thermal conductivity depends on temperature (e.g., see Refs. [18,19,20]). Thermal nonlinearity is a common phenomenon in engineering, but it is not widely studied in theory like nonlinear optics.

Metasurfaces (structural surfaces), which are actually two-dimensional metamaterials, have been an important part in the field of manipulating electromagnetic waves [21,22]. In this work, we propose a class of thermal metasurfaces, which are composed of a mixture of two different materials with different thermal conductivities. Especially, we focus on the cases where the heat conductivity of the inclusions or host is nonlinear, namely, dependent on temperature. We shall develop two methods to deal with this problem. First, we develop the effective medium theory for the thermal metasurfaces and investigate the enhancement effect of nonlinear heat transfer in metasurfaces. Then we develop the perturbation theory to handle the

situation of weak nonlinearity. This method helps us to reveal high-order harmonic frequencies of heat flux for a heat source with periodic temperature.

## 2 Effective medium theory for metasurfaces: Bruggeman and Maxwell-Garnett (M&G) formulas

Firstly, we use the effective medium theory to study the mixing rules in our thermal metasurface, which has been attempted in the research of electromagnetic meta (e.g., see Ref. [23]). According to the M&G and Bruggeman theory, the effective thermal conductivity  $\kappa_e$  of a thermal metasurface consisting of two materials A and B can be described by [24]

$$\frac{\kappa_e - \kappa_B}{\kappa_e + \kappa_B} = p_A \frac{\kappa_A - \kappa_B}{\kappa_A + \kappa_B}, \quad (1a)$$

$$\frac{\kappa_e - \kappa_A}{\kappa_e + \kappa_A} = p_B \frac{\kappa_B - \kappa_A}{\kappa_B + \kappa_A}, \quad (1b)$$

$$p_A \frac{\kappa_e - \kappa_A}{\kappa_e + \kappa_A} + p_B \frac{\kappa_e - \kappa_B}{\kappa_e + \kappa_B} = 0, \quad (1c)$$

where  $\kappa_j$  and  $p_j$  stand for the thermal conductivity and area fraction of the  $j$ th component,  $j = A$  or  $B$ . Here  $p_A + p_B = 1$ . The above three equations are corresponding to the three conditions shown in Figure 1.

In order to show the validity of equation (1) in heat transfer, we compare the theoretical results predicted from equation (1) with the simulation results obtained from the finite-element method (FEM). Based on the structure

<sup>a</sup> e-mail: [jphuang@fudan.edu.cn](mailto:jphuang@fudan.edu.cn)

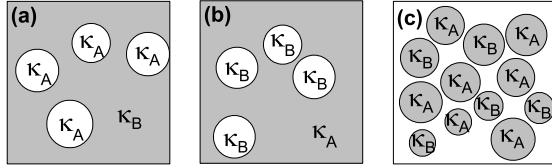


**Fig. 1.** Schematic diagram showing a mixture of two different materials A and B, with thermal conductivity  $\kappa_A$  and  $\kappa_B$ , respectively. The first two conditions correspond to the M&G theory with (a) circular particles A embedded in host medium B [based on Eq. (1a)] and (b) circular particles B embedded in host medium A [based on Eq. (1b)]. (c) The Bruggeman theory with circular particles occupying the whole space [based on Eq. (1c)].

shown in Figure 1a (M&G theory) and Figure 1c (Bruggeman theory), taking polydimethylsiloxane and coalesced copper (T2) as an example of material A and B respectively, we perform the FEM simulation for different area fractions. The size of the square box for simulation is set to be  $5\text{ cm} \times 5\text{ cm}$ , which contains more than 500 circles. As is shown in Figure 2, the corresponding simulation results are in agreement with the theoretical ones. The small discrepancy between theory and simulation may be due to the non-uniform distribution of circular particles, which can be overcome by utilizing a larger number of circles. The Bruggeman theory (red solid line) shown in Figure 2 echoes with the well-known percolation theory. Here polydimethylsiloxane can be regarded as heat insulation when compared with coalesced copper whose thermal conductivity is  $400\text{ W}/(\text{m}\cdot\text{K})$ . So, the critical point should be close to the area fraction of 0.5. And the big error bar located at  $p_A = 0.5$  corresponds to a large fluctuation near the critical point. This theory does not qualitatively classify two materials as conductive and insulating, but quantitatively describe two materials using different thermal conductivities. So, it can be seen as a more general version of percolation theory for the system under our consideration.

### 3 Nonlinearity enhancement: the enhancement of temperature coefficient

Now, the validity of equation (1) has been shown by the FEM simulations, in which the thermal conductivities are regarded as constants. However, for a real material, its thermal conductivity is thermally dependent more or less. Assuming the conductivity has a linear relationship with a given power of the temperature like

$$\kappa_A = \kappa_{A0} + \chi_A T^\alpha \quad \text{and} \quad \kappa_B = \kappa_{B0} + \chi_B T^\beta, \quad (2)$$

where  $\alpha$  and  $\beta$  can be any real number, we may express the effective thermal conductivity  $\kappa_e$  as

$$\kappa_e = \kappa_{e0} + c_1 \chi_A T^\alpha + c_2 \chi_B T^\beta + O(T^{2\alpha}) + O(T^{2\beta}). \quad (3)$$

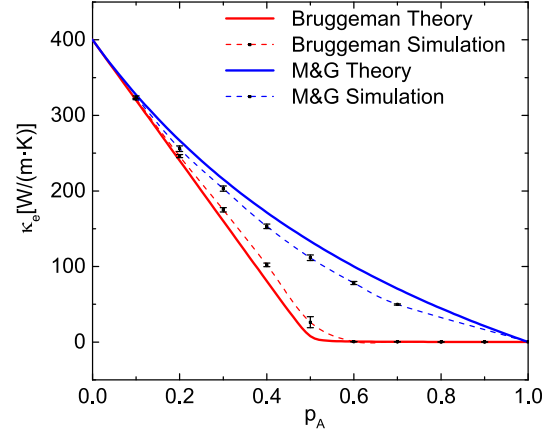


**Fig. 2.** Effective thermal conductivity  $\kappa_e$  versus area fraction  $p_A$  of polydimethylsiloxane [ $0.15\text{ W}/(\text{m}\cdot\text{K})$ , denoted as material A], for structures shown in Figures 1a and 1c. Here material B is coalesced copper (T2) [ $400\text{ W}/(\text{m}\cdot\text{K})$ ]. The bar associated with the symbols denotes the standard deviation.

Taking the Bruggeman equation as an example, we use equation (1c) to determine the parameters as

$$\kappa_{e0} = \frac{1}{2} \left[ \sqrt{(2p_A \kappa_{A0} - 2p_A \kappa_{B0} - \kappa_{A0} + \kappa_{B0})^2 + 4\kappa_{A0} \kappa_{B0}} + 2p_A \kappa_{A0} - 2p_A \kappa_{B0} - \kappa_{A0} + \kappa_{B0} \right], \quad (4)$$

$$c_1 = \frac{1}{2} \left[ \frac{4p_A^2 \kappa_{A0} - 4p_A \kappa_{A0} - 4p_A^2 \kappa_{B0} + 4p_A \kappa_{B0} + \kappa_{A0} + \kappa_{B0}}{\sqrt{(2p_A \kappa_{A0} - 2p_A \kappa_{B0} - \kappa_{A0} + \kappa_{B0})^2 + 4\kappa_{A0} \kappa_{B0}}} + 2p_A - 1 \right] - \frac{8(\kappa_B - \kappa_{B0})(p_A^2 \kappa_{A0} \kappa_{B0} - p_A \kappa_{A0} \kappa_{B0})}{((2p_A \kappa_{A0} - 2p_A \kappa_{B0} - \kappa_{A0} + \kappa_{B0})^2 + 4\kappa_{A0} \kappa_{B0})^{3/2}}, \quad (5)$$

and

$$c_2 = \frac{1}{2} \left[ \frac{(1-2p_A)(2p_A \kappa_{A0} - 2p_A \kappa_{B0} - \kappa_{A0} + \kappa_{B0}) + 2\kappa_{A0}}{\sqrt{(2p_A \kappa_{A0} - 2p_A \kappa_{B0} - \kappa_{A0} + \kappa_{B0})^2 + 4\kappa_{A0} \kappa_{B0}}} + 2p_A - 1 \right]. \quad (6)$$

For the sake of convenience and without loss of generality, we assume the thermal dependence of  $\kappa_A$  is much larger than  $\kappa_B$ , i.e.  $\chi_A T^\alpha \gg \chi_B T^\beta$ . Thus,  $\kappa_B$  can be treated as a constant. That is,  $\chi_B$  vanishes and  $c_2$  is invalidated. And  $\kappa_e$  will be simplified as

$$\kappa_e = \kappa_{e0} + \chi_e T^\alpha + O(T^{2\alpha}), \quad (7)$$

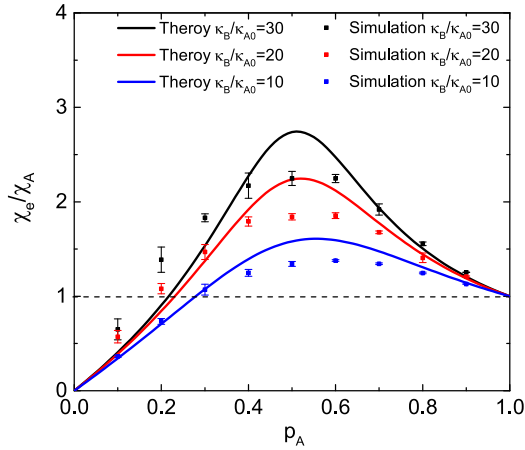


**Fig. 3.** Simulation results of nonlinearity enhancement effect based on Figure 1c/equation (1c). Ratio  $\chi_e/\chi_A$  as a function of  $p_A$  for different  $\kappa_B/\kappa_{A0}$ . As the ratio  $\chi_e/\chi_A$  is larger (or smaller) than 1, it represents nonlinearity enhancement (or reduction). The value of  $\chi_e/\chi_A$  obtained from theoretical calculation reaches maximum at  $p_A = 0.51, 0.52$  and  $0.56$  for  $\kappa_B/\kappa_{A0} = 30, 20$  and  $10$ , respectively. The simulation results (symbols) agree qualitatively with the theoretical ones (lines); the bar associated with the symbols denotes the standard deviation.

where

$$\kappa_{e0} = \frac{1}{2} \left[ \frac{\sqrt{(2p_A \kappa_{A0} - 2p_A \kappa_B - \kappa_{A0} + \kappa_B)^2 + 4\kappa_{A0} \kappa_B}}{+2p_A \kappa_{A0} - 2p_A \kappa_B - \kappa_{A0} + \kappa_B} \right], \quad (8)$$

$$\chi_e = \frac{1}{2} \chi_A \left[ \frac{(2p_A - 1) (2p_A \kappa_{A0} - 2p_A \kappa_B - \kappa_{A0} + \kappa_B) + 2\kappa_B}{\sqrt{(2p_A \kappa_{A0} - 2p_A \kappa_B - \kappa_{A0} + \kappa_B)^2 + 4\kappa_{A0} \kappa_B}} + 2p_A - 1 \right]. \quad (9)$$

Equation (9) can be rewritten as

$$\frac{\chi_e}{\chi_A} = \frac{1}{2} \left[ \frac{(2p_A - 1) \left( 2p_A - 2p_A \frac{\kappa_B}{\kappa_{A0}} - 1 + \frac{\kappa_B}{\kappa_{A0}} \right) + 2 \frac{\kappa_B}{\kappa_{A0}}}{\sqrt{\left( 2p_A - 2p_A \frac{\kappa_B}{\kappa_{A0}} - 1 + \frac{\kappa_B}{\kappa_{A0}} \right)^2 + 4 \frac{\kappa_B}{\kappa_{A0}}} + 2p_A - 1 \right]. \quad (10)$$

It is clear that the ratio of the nonlinear items, i.e.  $\chi_e/\chi_A$  only depends on the area fraction  $p_A$  and the ratio  $\kappa_B/\kappa_{A0}$ . After detailed calculation, the value of  $\chi_e/\chi_A$

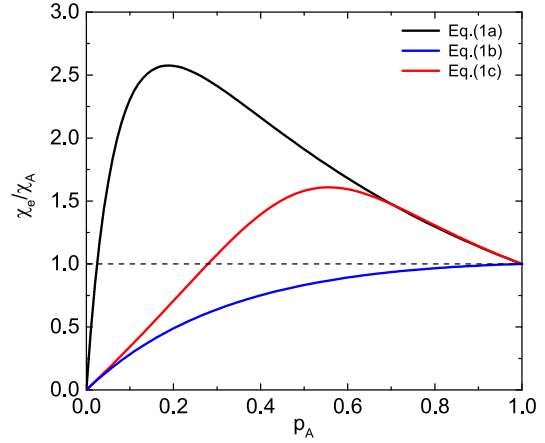


**Fig. 4.** Theoretical calculation of the ratio  $\chi_e/\chi_A$  versus  $p_A$  (area fraction of material A with temperature-dependant thermal conductivity) for  $\kappa_B/\kappa_{A0} = 10$ . The black, red and blue lines correspond to the conditions shown in Figure 1a/equation (1a), Figure 1c/equation (1c) and Figure 1b/equation (1b), respectively.

can exceed 1 under certain conditions. That is, the nonlinear item can be enhanced via the composite effect. In other words, the thermal dependence of a material can be stronger after mixing with a thermally independent material. As a model demonstration, the solid lines in Figure 3 exhibit the nonlinearity enhancement effects for different  $\kappa_B/\kappa_{A0}$  where we take  $\alpha = 1$  and  $\beta = 0$ . All the curves reach maximum around  $p_A = 0.5-0.6$ . We perform the FEM simulation to confirm the effect of nonlinearity enhancement; see the symbols in Figure 3. Despite a bias of peak position, the FEM simulation results repeat the enhancement effect indeed.

Till now, we have shown the enhancement effect produced by the Bruggeman theory [Fig. 1c/Eq. (1c)]. In fact, the M&G theory can also produce similar effects; see Figure 4. The comparison between Figure 1a/equation (1a) and Figure 1b/equation (1b) shows that the nonlinear coefficient can be largely enhanced when a normal host material B is embedded by a nonlinear material A, not vice versa.

#### 4 Perturbation theory for weak nonlinearity

So far we have used the effective-medium theory to compute the effective thermal conductivity of nonlinear composite media. Another method to deal with the problem is perturbation theory by analogy with nonlinear optics [25,26]. Now we consider a weak nonlinear relationship between thermal conductivity  $\kappa$  and temperature  $T$ , which can be generally expressed as

$$\kappa = \kappa_0 + \kappa_1 T + \kappa_2 T^2 + \kappa_3 T^3 + \dots, \quad (11)$$

where  $\kappa_n$  is the expansion parameters. To apply the perturbation theory, we should always have the following

condition,

$$|\kappa_0| \gg |\kappa_1 T| \gg |\kappa_2 T^2| \gg |\kappa_3 T^3| \gg \dots \quad (12)$$

The temperature itself can also be expanded as

$$T = T^{(0)} + T^{(1)} + T^{(2)} + T^{(3)} + \dots \quad (13)$$

Similarly, the expansion of heat flux  $\mathbf{J}$  is

$$\mathbf{J} = -(\kappa_0 + \kappa_1 T + \kappa_2 T^2 + \dots) \times \nabla(T^{(0)} + T^{(1)} + T^{(2)} + \dots). \quad (14)$$

Now we write the first three terms of heat flux as

$$\mathbf{J}^{(0)} = -\kappa_0 \nabla T^{(0)}, \quad (15)$$

$$\mathbf{J}^{(1)} = -\kappa_0 \nabla T^{(1)} - \kappa_1 T^{(0)} \nabla T^{(0)}, \quad (16)$$

and

$$\mathbf{J}^{(2)} = -\kappa_0 \nabla T^{(2)} - \kappa_1 T^{(0)} \nabla T^{(1)} - \kappa_1 T^{(1)} \nabla T^{(0)} - \kappa_2 (T^{(0)})^2 \nabla T^{(0)}. \quad (17)$$

Then we resort to Fourier's law of heat conduction,

$$\rho c \frac{\partial T}{\partial t} = \nabla \cdot (\kappa \nabla T), \quad (18)$$

where  $\rho$  is density and  $c$  is specific heat. Using the above expansions, we can get equations for every  $T^{(n)}$  (again we just write the first three terms),

$$\rho c \frac{\partial T^{(0)}}{\partial t} = \nabla \cdot (\kappa_0 \nabla T^{(0)}), \quad (19)$$

$$\rho c \frac{\partial T^{(1)}}{\partial t} = \nabla \cdot (\kappa_0 \nabla T^{(1)} + \kappa_1 T^{(0)} \nabla T^{(0)}), \quad (20)$$

and

$$\rho c \frac{\partial T^{(2)}}{\partial t} = \nabla \cdot (\kappa_0 \nabla T^{(2)} + \kappa_1 T^{(0)} \nabla T^{(1)} + \kappa_1 T^{(1)} \nabla T^{(0)} + \kappa_2 (T^{(0)})^2 \nabla T^{(0)}). \quad (21)$$

Now we consider a simple case, namely, embedding a nonlinear circular inclusion of radius  $r_i$  into a linear host medium. This corresponds to a two-dimensional steady-state question. The boundary condition at  $r = r_i$  is

$$\begin{cases} T_m^{(k)} = T_i^{(k)} \\ \mathbf{J}_m^{(k)} \cdot \hat{\mathbf{n}} = \mathbf{J}_i^{(k)} \cdot \hat{\mathbf{n}}, \end{cases} \quad (22)$$

where  $\hat{\mathbf{n}}$  is the unit normal vector on the surface of the inclusion. And the boundary condition at  $r = \infty$  and  $r = 0$

is set as

$$\begin{cases} \nabla T_m(r = \infty) = H e_x \\ |T_i^{(k)}(r = 0)| < \infty. \end{cases} \quad (23)$$

Here  $T_i$  and  $\mathbf{J}_i$  denote temperature and heat flux density of inclusion respectively and  $T_m$  and  $\mathbf{J}_m$  represent those of host medium. In addition, we take  $H$  as a given number.

The 0th-order solution is

$$\begin{cases} T_m^{(0)} = \frac{G}{r} \cos \theta + Hr \cos \theta \\ T_i^{(0)} = Cr \cos \theta, \end{cases} \quad (24)$$

where

$$\begin{cases} G = Hr_i^2 \frac{\kappa_m^{(0)} - \kappa_i^{(0)}}{\kappa_m^{(0)} + \kappa_i^{(0)}} \\ C = 2H \frac{\kappa_m^{(0)}}{\kappa_m^{(0)} + \kappa_i^{(0)}}. \end{cases} \quad (25)$$

Here we neglect the constant term in temperature which can take any realistic values and this will not influence any results below.

The 1st-order equation is

$$\nabla^2 T_i^{(1)} = -\frac{\kappa_i^{(1)}}{\kappa_i^{(0)}} C^2. \quad (26)$$

To solve such a non-homogeneous equation, we first find a special solution

$$-\frac{\kappa_i^{(1)}}{4\kappa_i^{(0)}} C^2 r^2 \quad (27)$$

and then set

$$\begin{cases} T_m^{(1)} = \frac{D}{r^2} \cos 2\theta \\ T_i^{(1)} = Er^2 \cos 2\theta - \frac{\kappa_i^{(1)}}{4\kappa_i^{(0)}} C^2 r^2 + F. \end{cases} \quad (28)$$

Finally we obtain

$$\begin{cases} F = \frac{\kappa_i^{(1)}}{4\kappa_i^{(0)}} C^2 r_i^2 \\ D = -\frac{C^2}{4} \frac{\kappa_i^{(1)}}{\kappa_i^{(0)} + \kappa_m^{(0)}} r_i^4 \\ E = -\frac{C^2}{4} \frac{\kappa_i^{(1)}}{\kappa_i^{(0)} + \kappa_m^{(0)}}. \end{cases} \quad (29)$$

To calculate the effective expansion parameters for  $\kappa$  in the whole system, we define a constitutive relationship between average heat flux and average thermal field as

$$\langle \mathbf{J} \rangle = -\kappa_e \langle \nabla T \rangle - \chi_e \langle T \rangle \langle \nabla T \rangle. \quad (30)$$

Following the method adopted in references [27,25], we write

$$\frac{1}{V} \int_V \mathbf{J} - (-\kappa_m^{(0)} \nabla T) d\Omega = \langle \mathbf{J} \rangle + \kappa_m^{(0)} \langle \nabla T \rangle. \quad (31)$$

Using equation (30) to replace  $\langle \mathbf{J} \rangle$  in the right-hand side of equation (31), we get

$$\begin{aligned} & \frac{1}{V} \int_{\Omega_i} ((\kappa_m^{(0)} - \kappa_i^{(0)}) \nabla T - \kappa_i^{(1)} T \nabla T) d\Omega \\ & = (\kappa_m^{(0)} - \kappa_e) \langle \nabla T \rangle - \chi_e \langle T \rangle \langle \nabla T \rangle. \end{aligned} \quad (32)$$

Substituting equation (24) into equation (32), we get

$$\kappa_e = \kappa_m^{(0)} - 2p_i \kappa_m^{(0)} \frac{\kappa_m^{(0)} - \kappa_i^{(0)}}{\kappa_m^{(0)} + \kappa_i^{(0)}}, \quad (33)$$

where  $p_i = \frac{\pi \rho^2}{V}$  is the area fraction of inclusion. Similarly, we can get

$$\chi_e = 2p_i \kappa_i^{(1)} \frac{\kappa_m^{(0)}}{\kappa_m^{(0)} + \kappa_i^{(0)}}. \quad (34)$$

Actually, when  $p_i \rightarrow 1$ , there should be  $\chi_e \rightarrow \kappa_i^{(1)}$ . This is because the condition, described by equation (12), is not valid in the whole area as  $|T(r = \infty)| = \infty$ . After all, in this case the nonlinearity is reduced, which is in accord with the results of effective medium theory. Although having the limitation of boundary conditions, the perturbation theory provides both approximate analytic temperature and another method to calculate effective heat conductivities.

## 5 Harmonic generation

Now let us focus on a one dimensional semi-infinite model with a periodic pulsing laser irradiating at position  $x = 0$ ; see Figure 5. Taking heat conductivity as  $\kappa = \kappa_0 + \chi_0 T^\alpha$ , the one-dimensional heat conduction equation is given by

$$\rho c \frac{\partial T}{\partial t} - \frac{d[(\kappa_0 + \chi_0 T^\alpha) \frac{dT}{dx}]}{dx} = 0. \quad (35)$$

According to the superposition principle, the temperature distribution can be expressed as

$$T(x, t) = T_{\text{amb}} + T_{\text{dc}}(x, t) + T_{\text{ac}}(x, t), \quad (36)$$

where  $T_{\text{amb}}$  is the ambient temperature taken as a constant,  $T_{\text{dc}}$  is the non-periodic time-dependent part, and  $T_{\text{ac}}$  is the periodic temperature with the same frequency  $\omega$  of heat source. For simplicity, we just set

$$T(x, t) = T^{(0)}, \quad (37)$$

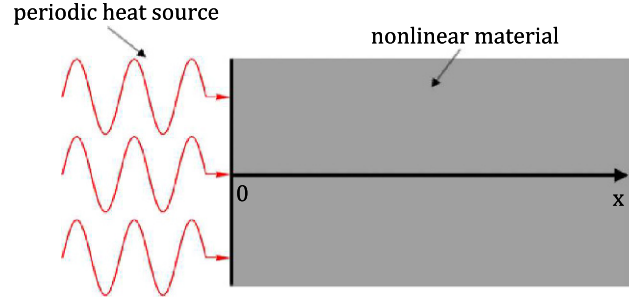


**Fig. 5.** Geometry of a one dimensional semi-infinite model for nonlinear heat transfer. The gray-colored space  $x > 0$  is filled by materials of nonlinear heat conductivity with a periodic heat source at position  $x = 0$ , illustrated as red wave lines.

which means neglecting  $\chi_0 T^\alpha$  in equation (35). Combining with the boundary condition, we obtain

$$J^{(0)}(x = 0) = J_{\text{dc}} + J_{\text{ac}} \cos(\omega t), \quad (38)$$

where  $J_{\text{dc}}$  and  $J_{\text{ac}}$  are the amounts of non-periodic and periodic heat flux at the source respectively. One can easily obtain [28]

$$T_{\text{dc}} = \frac{J_{\text{dc}}}{\sqrt{\kappa_0 \rho c}} \left( \frac{2\sqrt{t} e^{-\frac{x^2}{4\frac{\kappa_0}{\rho c} t}}}{\sqrt{\pi}} - \frac{\text{erfc}\left(\frac{x}{2\sqrt{\frac{\kappa_0}{\rho c} t}}\right)}{\sqrt{\frac{\kappa_0}{\rho c}}} x \right) \quad (39)$$

and

$$\begin{aligned} T_{\text{ac}}(x, t) &= \frac{J_{\text{ac}}}{\sqrt{\kappa_0 \rho c \omega}} e^{-\sqrt{\frac{\rho c \omega}{2\kappa_0}} x} \\ &\times \cos\left(\sqrt{\frac{\rho c \omega}{2\kappa_0}} x - \omega t + \pi/4\right), \end{aligned} \quad (40)$$

where  $\text{erfc}(x)$  is the error function. According to the perturbation theory, the heat flux distribution can be expressed as

$$\begin{aligned} J^{(0)} &= -\kappa_0 \frac{dT^{(0)}}{dx}, \\ J^{(1)} &= -\chi_0 (T^{(0)})^\alpha \frac{dT^{(0)}}{dx}. \end{aligned} \quad (41)$$

We can expect the existence of high-order harmonic heat flux in term  $J^{(1)}$ . It is also reasonable to expect that some new thermal effects can appear, such as sum frequency generation and difference frequency generation, which have been deeply studied in nonlinear optics.

In order to get an intuitive understanding of this high-order harmonic phenomenon, we take the alloy of gallium and indium (where the mass ratio of indium is 0.1) as an example, whose thermal conductivity may satisfy [29]

$$\begin{aligned} \kappa &= 7.2975 + 0.06716T \text{ [W/(m·K)]} \\ &\text{as } 303.15 \text{ K} < T < 363.15 \text{ K.} \end{aligned} \quad (42)$$

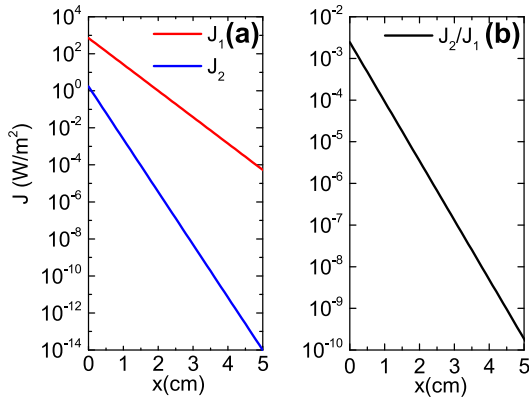


**Fig. 6.** Simulation results of nonlinear heat flux. The heat conductivity is set according to equation (42) and other parameters are  $\rho = 5940 \text{ kg/m}^3$ ,  $c = 1000 \text{ J/(kg}\cdot\text{K)}$ ,  $\omega = 1 \text{ s}^{-1}$  and  $J_{ac} = 1000 \text{ W/(m}^2\text{)}$ . (a) Absolute value of first-order and second-order harmonic heat flux,  $J_1$  and  $J_2$ , when  $x$  varies. (b) The ratio  $J_2/J_1$  as a function of  $x$ .

Dropping the direct item  $J_{dc}$  of input heat flux and writing the temperature in form of complex number,  $T = \text{Re}(\tilde{T})$  [here  $\text{Re}(\dots)$  is the real part of  $\dots$ ], we have

$$\tilde{T}(x, t) = T_{\text{amb}} + T_1(x)e^{-i\omega t}, \quad (43)$$

where

$$T_1 = \frac{J_{ac}}{\sqrt{\kappa_0 \rho c \omega}} e^{-\sqrt{\frac{\rho c \omega}{2\kappa_0}} x} e^{i\left(\sqrt{\frac{\rho c \omega}{2\kappa_0}} x + \pi/4\right)}. \quad (44)$$

Then, the expression of heat flux can be written as

$$J = \text{Re}(\tilde{J}_1 + \tilde{J}_2), \quad (45)$$

where

$$\begin{aligned} \tilde{J}_1 &= -(\kappa_0 + \chi_0 T_{\text{amb}}) \frac{dT_1}{dx} e^{-i\omega t}, \\ \tilde{J}_2 &= -\chi_0 T_1 \frac{dT_1}{dx} e^{-2i\omega t}. \end{aligned} \quad (46)$$

It can be seen that the temperature dependence of thermal conductivity will terminate the heat flux after a certain order. And we can get the amplitudes of first-order and second-order heat flux  $J_1 = \text{Re}(\tilde{J}_1)$  and  $J_2 = \text{Re}(\tilde{J}_2)$ ; see Figure 6. Clearly, both  $J_1$  and  $J_2$  decay exponentially in space (Fig. 6a) while  $J_2$  decays much faster than  $J_1$  (Fig. 6b).

## 6 Discussion and conclusions

In this work, the composite effect provides a simple but efficient way to control the nonlinear coefficient of heat conduction materials. Based on the above enhancement and reduction, we may design some useful structures. For example, due to the enhancement of the nonlinear coefficient, the composite will be more sensitive to the variation

of environment temperature. So, the enhancement region can be used for sensors, thermal switches, and so on. On the other hand, the reduction region can be used as thermal stabilizer by reducing the nonlinear coefficient. This can combine improved thermal performance with other excellent characteristics such as electronic, magnetic and mechanical properties. Also, a thermal diode can be a potential application. It is known that such rectification can be reached by tailoring the non-symmetrical properties of materials with temperature-dependent thermal conductivities. Here we suggest to add nonlinearity enhancement or reduction as an additional tuning parameter for optimizing the rectification.

To sum up, we have developed two methods, the effective medium theory and perturbation theory, to investigate thermal metasurfaces (structural surfaces). Based on the two theories, we have revealed the nonlinearity enhancement phenomenon due to the composite effect, and reported high-order harmonic heat waves generated in nonlinear thermal materials. These results provide new hints on designing novel thermal metamaterials or meta-devices, such as thermal diodes, sensors and switches, in order to control and manipulate the flow of heat. Furthermore, this work makes it possible to develop nonlinear thermotics on the same footing as nonlinear optics; the latter's focus is on all nonlinear optical responses including harmonic generation and nonlinearity enhancement (e.g., see Ref. [30]). But, from physical point of view, an essential difference between nonlinear thermotics (mentioned herein) and nonlinear optics lies in the fact that thermal conductivities in nonlinear thermotics depend on temperatures (rather than temperature gradients) while dielectric constants in nonlinear optics rely on electric fields (rather than electric potentials). Importantly, here the temperature (rather than the temperature gradient) is mathematically analogous to the electric potential (whose gradient yields electric fields), which indicates that a different theoretical framework needs to be established or developed for describing the different physical mechanism of nonlinear thermotics.

We acknowledge the financial support by the National Natural Science Foundation of China under Grant No. 11725521, and by the Science and Technology Commission of Shanghai Municipality under Grant No. 16ZR1445100.

## Author contribution statement

All the authors were involved in the preparation of the manuscript. All the authors have read and approved the final manuscript. J.H., G.D., and J.S. designed research; G.D., J.S., and R.W. performed research; and G.D., J.S., R.W., and J.H. wrote the paper.

## References

1. B. Li, L. Wang, G. Casati, Phys. Rev. Lett. **93**, 184301 (2004)
2. B. Li, L. Wang, G. Casati, Appl. Phys. Lett. **88**, 143501 (2006)

3. L. Wang, B. Li, Phys. Rev. Lett. **99**, 177208 (2007)
4. N. Li, J. Ren, L. Wang, G. Zhang, P. Hänggi, B. Li, Rev. Mod. Phys. **84**, 1045 (2012)
5. P. Ben-Abdallah, S.A. Biehs, Phys. Rev. Lett. **112**, 044301 (2014)
6. V. Kubyt'skiy, S.A. Biehs, P. Ben-Abdallah, Phys. Rev. Lett. **113**, 074301 (2014)
7. C.Z. Fan, Y. Gao, J.P. Huang, Appl. Phys. Lett. **92**, 251907 (2008)
8. T. Chen, C.N. Weng, J.S. Chen, Appl. Phys. Lett. **93**, 114103 (2008)
9. S. Narayana, Y. Sato, Phys. Rev. Lett. **108**, 214303 (2012)
10. R. Schittny, M. Kadic, S. Guenneau, M. Wegene, Phys. Rev. Lett. **110**, 195901 (2013)
11. H.Y. Xu, X.H. Shi, F. Gao, H.D. Sun, B.L. Zhang, Phys. Rev. Lett. **112**, 054301 (2014)
12. T.C. Han, X. Bai, D.L. Gao, J.T.L. Thong, B.W. Li, C.W. Qiu, Phys. Rev. Lett. **112**, 054302 (2014)
13. Y.G. Ma, Y.C. Liu, M. Raza, Y.D. Wang, S.L. He, Phys. Rev. Lett. **113**, 205501 (2014)
14. T.C. Han, X. Bai, J.T.L. Thong, B.W. Li, C.W. Qiu, Adv. Mater. **26**, 1731 (2014)
15. T.Z. Yang, X. Bai, D. Gao, L. Wu, B.W. Li, J.T.L. Thong, C.W. Qiu, Adv. Mater. **27**, 7752 (2015)
16. Y. Li, X.Y. Shen, Z.H. Wu, J.Y. Huang, Y.X. Chen, Y.S. Ni, J.P. Huang, Phys. Rev. Lett. **115**, 195503 (2015)
17. X.Y. Shen, Y. Li, C.R. Jiang, J.P. Huang, Phys. Rev. Lett. **117**, 055501 (2016)
18. S. Liu, X.F. Xu, R.G. Xie, G. Zhang, B.W. Li, Eur. Phys. J. B **85**, 337 (2012)
19. L.L. Yang, N.B. Li, B.W. Li, Phys. Rev. E **90**, 062122 (2014)
20. Y.Y. Li, N.B. Li, B.W. Li, Eur. Phys. J. B **88**, 182 (2015)
21. N. Yu, P. Genevet, M.A. Kats, F. Aieta, J.P. Tetienne, F. Capasso, Z. Gaburro, Science **334**, 333 (2011)
22. N. Yu, F. Capasso, Nat. Mater. **13**, 139 (2014)
23. O. Ouchetto, C.W. Qiu, S. Zouhdi, L.W. Li, A. Razek, IEEE Trans. Microw. Theory Tech. **54**, 3893 (2006)
24. J.P. Huang, K.W. Yu, Phys. Rep. **431**, 87 (2006)
25. G.Q. Gu, K.W. Yu, Phys. Rev. B **46**, 4502 (1992)
26. K.W. Yu, G.Q. Gu, Phys. Rev. B **46**, 4502 (1992)
27. L. Gao, J.P. Huang, K.W. Yu, Eur. Phys. J. B **36**, 475 (2003)
28. A. Salazar, Eur. J. Phys. **27**, 1349 (2006)
29. S.S. Zhang, Z.S. Deng, J. Liu, in *Conference on Heat and Mass Transfer of Chinese Society of Engineering Thermophysics, Dongguan, China* (2012), No. 123686 (in Chinese)
30. L. Gao, Phys. Rev. E **71**, 067601 (2005)